The Effect of Nonlinear Drag on the Motion and Settling Velocity of Heavy Particles

J. E. STOUT

Department of Agriculture/Agriculture Research Service, Lubbock, Texas

S. P. ARYA

Department of Marine, Earth, and Atmospheric Sciences, North Carolina State University, Raleigh, North Carolina

E. L. GENIKHOVICH*

Voeikov Main Geophysical Observatory, St. Petersburg, Russia

(Manuscript received 4 April 1994, in final form 14 March 1995)

ABSTRACT

The effects of nonlinear drag on the motion and settling velocity of heavy particles in a turbulent atmosphere are investigated. The authors approach the problem rather systematically by first considering the response of particles to much simpler fluid motions that are subprocesses of the more complex turbulent field. The authors first consider the motion and time response of particles falling under gravity in still fluid. Then the effects of a sudden gust or step change in relative velocity between a falling particle and its surrounding fluid are investigated. The authors demonstrate that horizontal relative motion produced by a sudden gust tends to reduce the settling velocity of a particle. In simple oscillating fluids it is shown that the reduction of settling velocity increases with increasing amplitude of fluid oscillation. The authors also explore the effects of oscillation frequency on the settling velocity and show that if the period of fluid oscillation is less than the particle response time, then the settling velocity reduction becomes independent of oscillation frequency. Finally, the authors explore the motion of heavy particles within simulated isotropic turbulence and show that the effect of nonlinear drag is to produce a slowing of particle settling velocity.

1. Introduction

A heavy particle is one that has a larger density than the surrounding fluid so that within a gravitational field it is negatively buoyant. Both a large raindrop and a small dust speck qualify as heavy particles, but their behavior in turbulent flow can be quite different. Past work has defined at least three fairly distinct regimes of heavy particle motion that depend primarily on the ratio of the velocity scale of the fluid σ to the terminal velocity of the particle W_T. The regimes are depicted in Fig. 1.

If $\sigma/W_T \gg 1$, which corresponds to vigorous fluid motions and small particles with little inertia, Stommel (1949) and Manton (1974) have shown that particles will often follow closed trajectories in idealized turbulent eddies and thereby remain suspended. In reality smaller-scale turbulent fluctuations tend to reduce this eddy-trapping effect, but the average settling velocity of particles can be greatly reduced in this regime.

For $\sigma/W_T \approx 1$, which corresponds to somewhat larger particles and less vigorous fluid motions, Maxey and Corrsin (1986), Maxey (1987), and Wang and Maxey (1993) have shown that particles with small to moderate inertia tend to move outward from the center of eddies and are often preferentially swept into regions of downdrafts where they may actually settle out more rapidly than in still fluid. In this regime a small net increase in settling velocity has been observed in numerical simulations, but this result has not been confirmed experimentally.

Finally for $0 < \sigma/W_T \ll 1$, which corresponds to large and heavy particles in relatively weak fluid motions, particles pass rapidly and quite vertically through turbulent eddies, where they experience a series of fluid gusts as they fall. For sufficiently large particles the timescale of the fluid velocity fluctuations can be much smaller than the response time of the particles, and the net effect is a substantial amount of relative motion between the particle and the fluid. For particles falling in the nonlinear drag regime substantial relative motion

* Current affiliation: Atmospheric Research and Exposure Assessment Laboratory, U.S. Environmental Protection Agency, Research Triangle Park, North Carolina.

Corresponding author address: Dr. John E. Stout, USDA/ARS, Route 3, Box 215, Lubbock, TX 79401.
E-mail: jstout@lubbock.ars.ag.gov

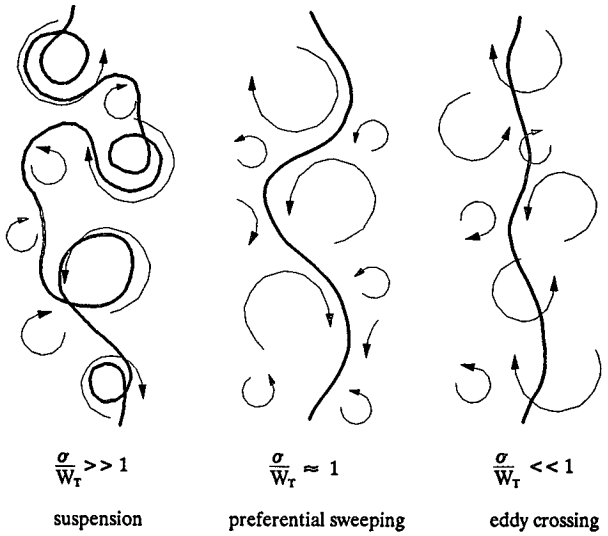

FIG. 1. Three regimes of heavy particle motion.

can produce an appreciable upward force on each particle, thereby slowing the rate of descent. This nonlinear drag effect has been observed in experiments of particles falling through vertically oscillating fluids by Tunstall and Houghton (1968) and Schöneborn (1975). In addition, Laws (1941) has observed large raindrops to fall more slowly in atmospheric turbulence than in still air, perhaps due to this nonlinear drag effect.

The primary goal of this work is to explore the effect of nonlinear drag on the motion of heavy particles falling through moving fluids, especially turbulent fluids, by calculating the motion of individual particles. The prediction of particle motion is based upon equations that predict the natural reaction of particles to applied fluid dynamic and gravitational forces. We begin our investigation by first considering the response of particles to simple fluid motions that represent subprocesses of the more complex turbulent flow. The simplest case considered is a particle falling through a still fluid. Then a sustained gust is introduced, and the transient response of the particle is computed. Next, the response of a falling particle to sinusoidal fluid motions is considered, and the effects of oscillation amplitude and frequency are investigated. Finally, we explore the motion and settling velocity of heavy particles falling through a simulated field of isotropic turbulence.

2. Equations of particle motion

The horizontal, lateral, and vertical coordinates are denoted (x, y, z) with unit vectors $(\mathbf{i}, \mathbf{j}, \mathbf{k})$. The coordinate system is oriented so that the gravitational vector acts parallel to the z-axis in the $-\mathbf{k}$ direction. The particle velocity vector is $\mathbf{V}_p = (u_p, v_p, w_p)$, and the fluid velocity at the position of the particle is $\mathbf{V} = (u, v, w)$. The relative velocity vector is $\mathbf{V}_{\text{rel}} = \mathbf{V} - \mathbf{V}_p$, which is the fluid velocity as seen by an observer moving with the particle. The relative wind vector has components $\mathbf{V}_{\text{rel}} = (u_{\text{rel}}, v_{\text{rel}}, w_{\text{rel}})$.

Drag of spherical particles

The drag of spherical particles has been studied extensively in the past. In its most general form the drag force vector may be expressed as

$$\mathbf{F} = C_D \frac{\pi D^2}{8} \rho V_{\text{rel}} \mathbf{V}_{\text{rel}}, \tag{1}$$

where C_D is the drag coefficient, D is the diameter of the particle, ρ is the fluid density, and V_{rel} is the magnitude of the resultant relative velocity vector $\mathbf{V}_{\text{rel}}$. The drag coefficient C_D is primarily a function of Reynolds number, which may be expressed as

$$\text{Re} = \frac{\rho V_{\text{rel}} D}{\mu}, \tag{2}$$

where μ is the absolute viscosity of the fluid.

For $\text{Re} \ll 1$, called the Stokes regime, $C_D = 24/\text{Re}$, and Eq. (1) reduces to linear form. In other words, the fluid drag forces are linearly proportional to the relative velocity between the particle and fluid. For a larger Reynolds number, $\text{Re} \gg 1$, fluid drag is nonlinear. This fundamental difference in the drag force has an important effect on particle behavior in moving fluids, and it is this nonlinear effect on particle motion that is of interest here.

The drag of spherical particles has been measured by numerous experimentalists, and a substantial portion of these data have been summarized by Zahm (1926) and Hoerner (1958). A plot of measured values of C_D as a function of Re from Zahm (1926) is shown in Fig. 2. Below the critical Reynolds number ($\text{Re} < 10^5$), the data points fall near a well-defined curve, called the standard drag curve. The standard drag curve has been tabulated by Clift et al. (1978). Numerous empirical equations have been proposed to describe the standard drag curve (e.g., Kladas and Georgiou 1993).

White (1974) proposed a simple empirical formula for calculating the drag coefficient of a sphere over a wide range of Reynolds number. The drag equation is expressed as

$$C_D = c_1 + \frac{24}{\text{Re}} + \frac{c_2}{1 + \sqrt{\text{Re}}}. \tag{3}$$

For $\text{Re} < 5 \times 10^3$, good agreement is found when $c_1 = 0.25$ and $c_2 = 6$, as shown in Fig. 2.

Particles are assumed to be spherical with density ρ_p, and we restrict our consideration to heavy particles with $\rho_p \gg \rho$. It is easily shown that for such heavy particles terms involving the pressure gradient force, the virtual mass force, and the Basset force can be ne-

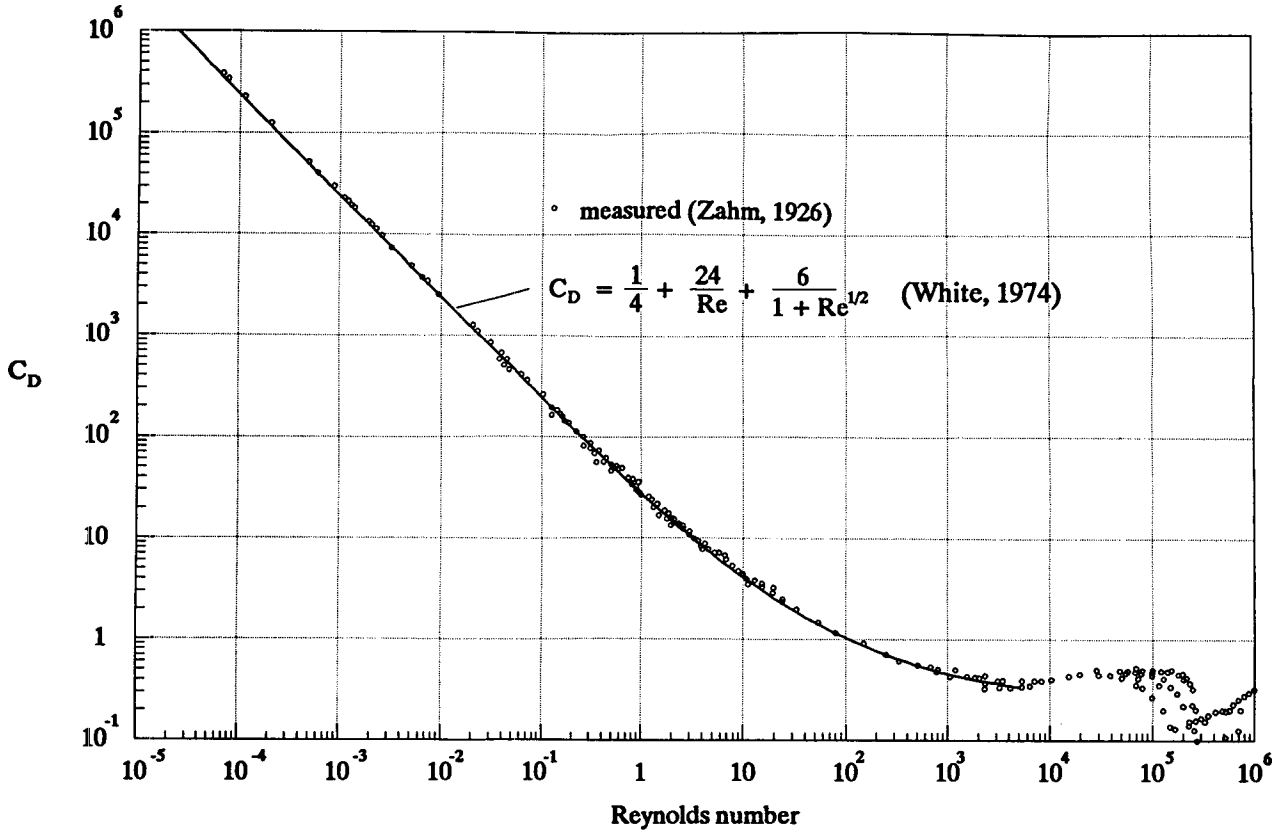

FIG. 2. Drag measurements compiled by Zahm (1926) compared with the empirical equation proposed by White (1974).

glected; and the equation governing particle motion reduces to the following form:

$$\frac{d\mathbf{V}_p}{dt} = \frac{3}{4}\frac{\rho}{\rho_p}\frac{C_D}{D} V_{\text{rel}}\mathbf{V}_{\text{rel}} - g\frac{\rho_p - \rho}{\rho_p}\mathbf{k}. \quad (4)$$

The motion of each particle is calculated by an explicit scheme that is iterated over many small time steps Δt (Stout et al. 1993). The particle velocity as a function of time is calculated as

$$(\mathbf{V}_p)_{\tau+1} = (\mathbf{V}_p)_\tau + \left(\frac{d\mathbf{V}_p}{dt}\right)_\tau \Delta t, \quad (5)$$

where the subscript τ denotes the time step. Particles are released with known initial velocity. The velocity of the particle at time step $\tau + 1$ is computed from values of particle velocity and particle acceleration at time step τ. Particle acceleration is calculated from Eq. (4) from known values of relative velocity at time step τ.

An alternate form of the equation of motion is obtained for the case of a still fluid or a steady and spatially uniform flow. In this case the fluid velocity is unchanged following the particle or $d\mathbf{V}/dt = 0$, and the equation of motion can be rewritten in terms of the relative velocity instead of the particle velocity as

$$\frac{d\mathbf{V}_{\text{rel}}}{dt} = g\frac{\rho_p - \rho}{\rho_p}\mathbf{k} - \frac{3}{4}\frac{\rho}{\rho_p}\frac{C_D}{D} V_{\text{rel}}\mathbf{V}_{\text{rel}}. \quad (6)$$

This equation is not valid for particles experiencing unsteady flow.

3. Vertical motion in a still fluid

Consider the motion of a particle released from rest in a still fluid. In this case, $u_{\text{rel}} = v_{\text{rel}} = 0$, and Eq. (6) reduces to

$$\frac{dw_{\text{rel}}}{dt} = g\frac{\rho_p - \rho}{\rho_p} - \frac{3}{4}\frac{\rho}{\rho_p}\frac{C_D}{D}|w_{\text{rel}}|w_{\text{rel}}. \quad (7)$$

The relative velocity as a function of time is calculated as

$$(w_{\text{rel}})_{\tau+1} = (w_{\text{rel}})_\tau + \left(\frac{dw_{\text{rel}}}{dt}\right)_\tau \Delta t. \quad (8)$$

The drag coefficient is adjusted at each time step using White's drag equation with $c_1 = 0.25$ and $c_2 = 6$.

a. *Terminal velocity*

When released, particles naturally accelerate until the gravitational force is balanced by drag, at which

point the velocity of the particle relative to the fluid becomes constant. The final steady value of w_{rel} is called the terminal velocity W_T. By setting Eq. (7) equal to zero and solving for w_{rel}, we obtain the definition of W_T as

$$W_T \equiv \left(\frac{4}{3}\frac{D}{C_{D_T}} g \frac{\rho_p - \rho}{\rho}\right)^{1/2}. \quad (9)$$

Note that we designate C_{DT} as the drag coefficient of the particle when falling at terminal velocity. Similarly, we define the terminal Reynolds number Re_T as the Reynolds number of the particle when falling at terminal velocity as

$$\mathrm{Re}_T \equiv \frac{\rho W_T D}{\mu}. \quad (10)$$

Model predictions of Re_T, C_{DT}, and W_T for falling droplets are shown in Table 1 along with experimental values from Gunn and Kinzer (1949). The rms error is less than 3%. It is not surprising that there is good agreement between the model and these experimental values since the drag coefficient of spherical particles was derived from similar experiments. The disagreement at large D is mainly associated with the deformation of the water drop from spherical shape (e.g., Mason 1957).

b. Time history of fall

Properly simulating the terminal velocity is important, but the same value of terminal velocity can be obtained from an improper simulation of the time history of fall. For a particle falling within the Stokes regime the time history of fall can be obtained analytically (Fuchs 1964). The derivation is shown in the appendix, and the final solution is

$$\frac{w_{rel}(t)}{W_T} = 1 - e^{-t/\tau_s}, \quad (11)$$

where

$$\tau_s \equiv \frac{\rho_p D^2}{18\mu}. \quad (12)$$

As a large and heavy particle accelerates from rest, the gravitational force is initially so much larger than the drag force that the latter is negligible. Thus, during the initial phases of acceleration, the drag term is relatively small, and the proper value of C_D is not critical. If by the time the drag term becomes comparable to the gravitational term the Reynolds number is in the range $10^2 < \mathrm{Re} < 10^4$, then for all practical purposes the value of C_D will have nearly reached its final value of C_{DT}. Thus, for particles with terminal Reynolds number within the range $10^2 < \mathrm{Re}_T < 10^4$, the approximation $C_D \approx C_{DT}$ may be sufficient. With such an assumption, we can solve Eq. (7) for the time history of fall within the nonlinear drag regime. The full derivation is shown in the appendix, and the final solution is

$$\frac{w_{rel}(t)}{W_T} = \tanh(t/\tau_p), \quad (13)$$

where

$$\tau_p \equiv W_T \Big/ g\frac{\rho_p - \rho}{\rho_p}. \quad (14)$$

The ratio of the timescales is

$$\frac{\tau_s}{\tau_p} = \frac{\mathrm{Re}_T C_{DT}}{24}. \quad (15)$$

TABLE 1. Model predictions of Re_T, C_{DT}, and W_T for water droplets compared with experimentally measured values from Gunn and Kinzer (1949).

	Model			Experiment[a]			
D (μm)	Re_T	C_{DT}	W_T (m s^{-1})	Re_T	C_{DT}	W_T (m s^{-1})	τ_p (s)
100	1.7	17.3	0.25	1.8	14.8	0.27	0.028
200	9.5	4.24	0.71	9.6	4.18	0.72	0.073
300	23.9	2.28	1.19	23.4	2.37	1.17	0.119
400	44.1	1.58	1.66	43.1	1.65	1.62	0.165
500	69.6	1.24	2.09	68.6	1.28	2.06	0.210
600	100.0	1.04	2.50	98.7	1.06	2.47	0.252
700	134.9	0.903	2.90	133.7	0.920	2.87	0.293
800	174.0	0.811	3.27	174.2	0.810	3.27	0.334
900	217.1	0.742	3.62	219.9	0.723	3.67	0.375
1000	263.9	0.689	3.96	268.3	0.666	4.03	0.411
1200	367.8	0.613	4.60	370.7	0.603	4.64	0.474
1400	484.7	0.560	5.20	481.9	0.567	5.17	0.528
1600	613.5	0.522	5.76	601.8	0.542	5.65	0.577
1800	753.4	0.493	6.29	729.8	0.525	6.09	0.622
2000	903.8	0.470	6.79	864.1	0.514	6.49	0.662

[a] $\mu = 1.81 \times 10^{-5}$ kg m^{-1} s^{-1}, $\rho = 1.205$ kg m^{-3} (air), and $\rho_p = 998.2$ kg m^{-3} (water).

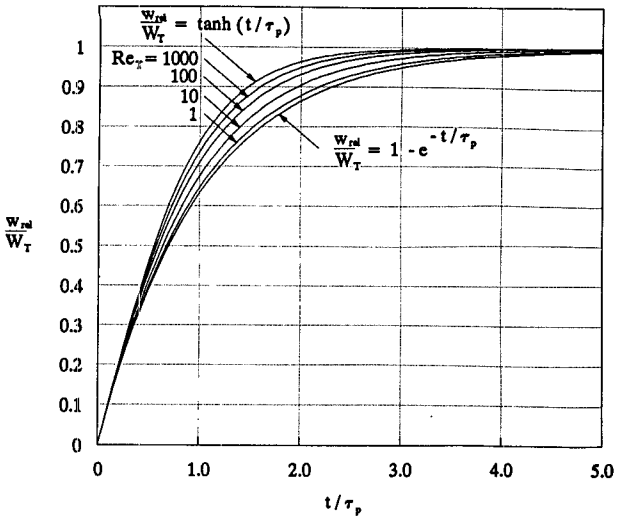

FIG. 3. Numerical and analytical predictions of the vertical relative velocity of a particle falling through a still fluid.

If $Re_T \ll 1$, then $C_{DT} = 24/Re_T$, and we find that $\tau_s = \tau_p$. On the other hand, if $Re_T \gg 1$, then τ_s and τ_p diverge significantly because τ_s is not a valid timescale within the nonlinear drag regime. Calculated τ_p values for various-diameter water drops based upon their terminal fall velocity as measured by Gunn and Kinzer (1949) are shown in the last column of Table 1.

A plot of Eqs. (11) and (13), along with numerical solutions for various values of Re_T, are shown in Fig. 3. Equation (11) is the limiting case for small Re_T, and Eq. (13) appears to be the limiting case for large Re_T. These two analytical solutions form an envelope within which all other time history curves fall.

For heavy particles with intermediate terminal Reynolds number, say $1 < Re_T < 10^3$, neither analytical expression adequately describes the time history of fall. To obtain a proper time history with a correct simulation of $C_D(Re)$, it is necessary to solve Eq. (7) numerically. The numerical results are then compared with experimentally measured data from Laws (1941).

Laws (1941) measured the fall velocity of water drops as a function of height of fall. Running the model for exactly the same conditions, a comparison is made with these measurements. The results for 1.19- and 1.74-mm diameter water drops are compared with numerical predictions in Fig. 4. Generally, the results show good agreement, indicating that the model is capable of adequately simulating the time history of fall in still fluid.

4. Response of a particle to a step change in relative motion

In the previous section we investigated the motion of particles falling with no horizontal relative motion. A particle falling vertically through a still fluid or a particle drifting along in a uniform and steady flow are examples of such motion. In this section we consider the response of a falling particle when subjected to a step change in either horizontal or vertical relative motion. A particle subjected to a sudden fluid gust and a particle released with an impulsive velocity in a still fluid are dynamically equivalent. Both cases are considered simultaneously by solving for the relative velocity instead of the particle velocity.

a. Nondimensional form of the equation of particle motion

At this point it is more convenient to work with the nondimensional form of the governing equation of motion. Selecting the particle time constant τ_p as a timescale [see Eq. (14)] and the terminal velocity W_T as a velocity scale [see Eq. (9)], the governing equation of motion may be written in the following nondimensional form:

$$\frac{d\mathbf{V}^*_{rel}}{dt^*} = \mathbf{k} - \frac{C_D}{C_{D_T}} V^*_{rel}\mathbf{V}^*_{rel}, \qquad (16)$$

where asterisks denote a nondimensional variable. To solve this equation, we need only specify the value of one nondimensional constant, Re_T. The value of C_{DT} is determined from the value of Re_T through White's drag equation [Eq. (3)]. We can also write Re in terms of Re_T as follows:

$$Re = Re_T V^*_{rel}. \qquad (17)$$

Thus, both C_D and C_{DT} can be written as functions of Re_T.

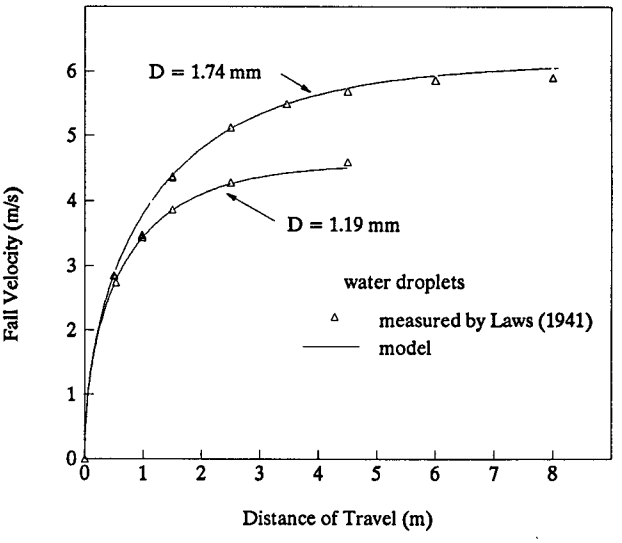

FIG. 4. Fall velocity of water droplets within still air as a function of travel distance (Laws 1941) compared with the model.

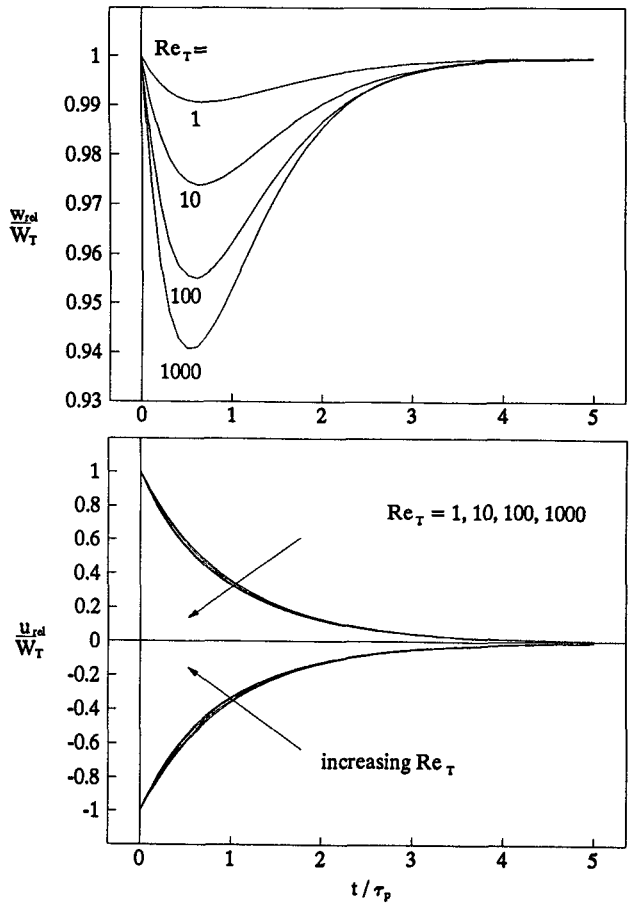

FIG. 5. Response of a particle to a step change of horizontal relative motion.

b. Step change in horizontal relative motion

In the nonlinear drag regime the response of a falling particle to a sudden and sustained horizontal gust is quite interesting and complicated. For example, consider a particle falling vertically through a fluid when it suddenly encounters either a positive or negative horizontal gust equal in magnitude to its terminal velocity. The initial conditions are $u_{\text{relo}}/W_T = \pm 1$, $v_{\text{relo}}/W_T = 0$, and $w_{\text{relo}}/W_T = 1$. We calculate the response of the particle by solving Eq. (16) with $\text{Re}_T = 1$, 10, 100, and 1000.

The results, plotted in Fig. 5, show that the particle adjusts horizontally so as to reduce the initial horizontal relative motion to zero. As the particle adjusts, the vertical relative motion is momentarily reduced. The maximum reduction of w_{rel} increases with increasing Re_T. After an elapsed time of approximately three particle time constants, the vertical relative velocity has essentially returned to the still air terminal velocity as the particle now translates horizontally with the fluid.

To understand this lift effect caused by a horizontal gust, it is useful to examine more closely the governing equation of motion. The vertical component of drag is proportional to the product $C_D V_{\text{rel}} w_{\text{rel}}$. The magnitude of the total relative velocity vector V_{rel} increases as a sudden horizontal gust increases the component u_{rel}. This has the effect of increasing the vertical component of drag. The reduction of C_D with an increase of V_{rel} tends to counter this effect. For example, in the Stokes regime C_D is inversely proportional to V_{rel}, so that there is no net increase in the vertical component of drag due to a horizontal gust. But as the Reynolds number increases, the variation of C_D becomes less of a factor. Thus, a horizontal gust can significantly increase the net vertical force on a particle, slowing its downward motion through the fluid.

c. Step change in vertical relative motion

In this case we calculate the response of a particle to a step change in w_{rel}. We consider two cases: an upward fluid gust that initially doubles w_{rel} and a downward gust that initially reduces w_{rel} to zero. We calculate the response of the particle by solving Eq. (16). In this case the horizontal relative velocity remains zero during either gust. The results, plotted in Fig. 6, show that regardless of the sign of the initial value of w_{rel} the particle naturally adjusts so that it eventually falls with terminal velocity relative to the fluid after an elapsed time of approximately three particle time constants.

There is noticeable asymmetry in this figure due to the fact that the response of a particle to an upward gust is not the same as that to a downward gust. For the sake of argument, consider a particle falling with $\text{Re} \approx 10^4$ so that the variation of C_D with V_{rel} is negligible. For vertical motion only the vertical component of drag is proportional to $C_D w_{\text{rel}}^2$. For the case of an upward vertical gust that doubles w_{rel}, the upward component of

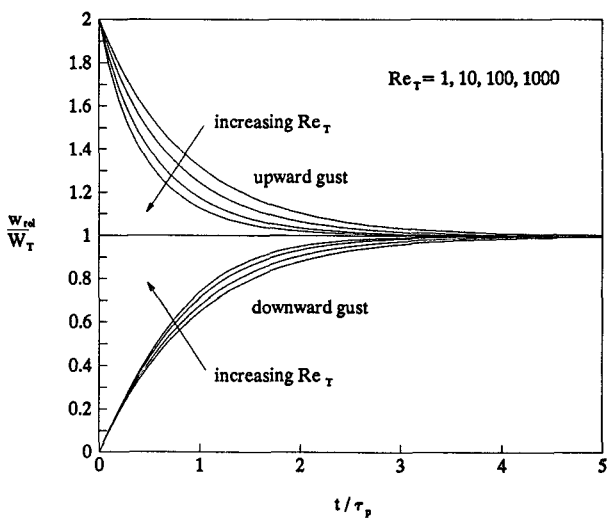

FIG. 6. Response of a particle to a step change of vertical relative motion.

drag increases momentarily by a factor of 4. For the opposite case of a downward vertical gust that reduces w_{rel} to zero, the upward component of drag reduces to zero. Herein lies the asymmetry of the fluid forcing when a particle is falling in the nonlinear drag regime. From this simple example it is easily deduced that, after a series of vertical gusts of both signs, the particle settling velocity will be reduced.

d. Conclusions

As expected, the natural reaction of a particle to either a vertical or a horizontal step change in relative velocity is to adjust so that $u_{rel}/W_T \to 0$ and $w_{rel}/W_T \to 1$. The time of adjustment is roughly three particle time constants. During the time of adjustment, a falling particle that encounters a horizontal gust will experience an enhanced vertical drag that slows its descent. A particle that encounters an upward gust will experience a larger net change in drag than a particle that encounters a downward gust of similar magnitude. Within a turbulent fluid, a particle will experience many gusts of different magnitude and duration, each producing both horizontal and vertical relative motion. Thus, one might expect that the average settling velocity would be reduced due to such gusts.

5. Particle motion in an oscillating fluid

In the previous section we investigated the motion of particles subjected to step changes in relative velocity. We found that, if given sufficient time, a particle subjected to such a step change eventually adjusts to follow the fluid horizontally and the settling velocity naturally adjusts to fall vertically with terminal velocity relative to the fluid. Now consider a fluid that continuously changes with time, so that the particle is unable to fully adjust to each fluid velocity fluctuation. We consider the case of either horizontal or vertical sinusoidal fluid oscillations, and we look at the effect of changing the amplitude or frequency of the fluid oscillations on the average settling velocity of the particle.

Since the particle is now falling through a flow field that varies with time following the particle ($d\mathbf{V}/dt \neq 0$), the nondimensional form of the equation of motion is

$$\frac{d\mathbf{V}_p^*}{dt^*} = \frac{C_D}{C_{D_T}} V_{\text{rel}}^* \mathbf{V}_{\text{rel}}^* - \mathbf{k}. \tag{18}$$

a. Vertically oscillating fluid

In this case we set all horizontal fluid velocity components to zero and allow the vertical component to vary with time as

$$w = W_0 \sin(2\pi n t), \tag{19}$$

where n is the frequency of fluid oscillations and W_0 is the amplitude.

The response of a particle as it falls through such an oscillating flow field is determined by solving Eq. (18). The particle is released with no horizontal motion and with a vertical velocity equal to the still air terminal velocity. A typical time trace for $W_0/W_T = 0.5$ and $n\tau_p = 10$ is shown in Fig. 7a. Note that the vertical velocity of the particle quickly becomes independent of the initial condition. It adjusts until it reaches a stable oscillation about a mean value that is less than unity. The adjustment time is approximately two particle time constants.

To determine the sensitivity of the settling velocity to the amplitude of vertical oscillation, the model is run for $0 \leq W_0/W_T \leq 1$. We limit our consideration to W_0/W_T less than or equal to unity so that the assumption of heavy and large particles is not violated. The final cycle-averaged settling velocity, denoted by a tilde, is calculated by averaging the particle velocity over at least one of the final cycles within the stable oscillation region. The results are shown in Fig. 8; each curve represents a different value of Re_T, which varies from 1 to 1000. As expected, the settling velocity decreases with increasing W_0/W_T, and for a fixed value of W_0/W_T the settling velocity decreases with increasing Re_T.

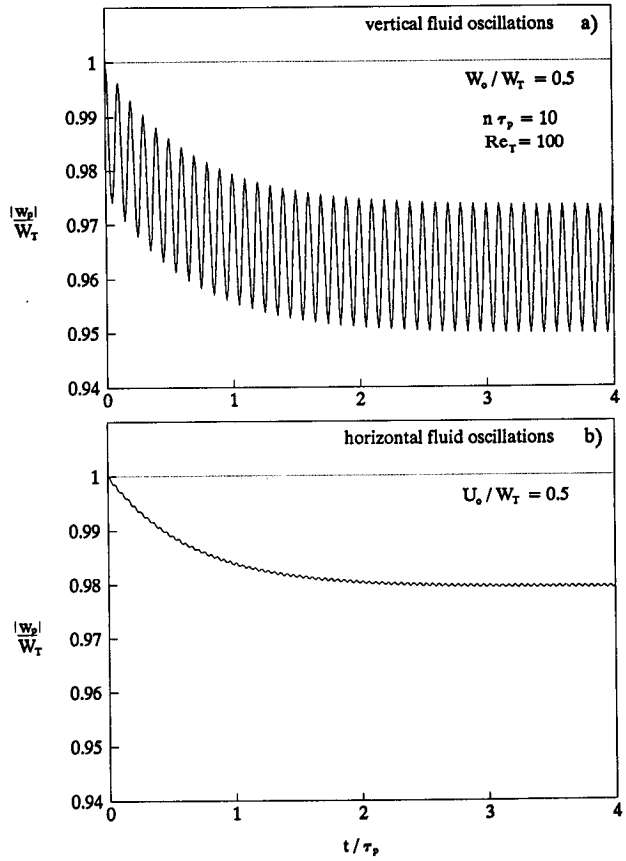

FIG. 7. Motion of a particle released within (a) vertically and (b) horizontally oscillating fluid.

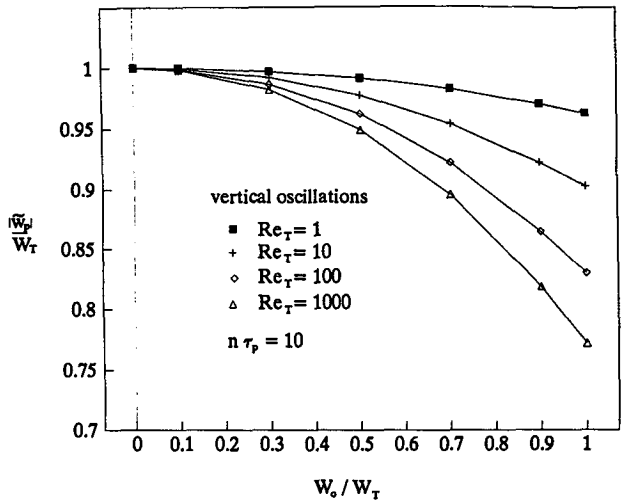

FIG. 8. Cycle-averaged settling velocity within a vertically oscillating fluid as a function of scaled oscillation amplitude and Re_T.

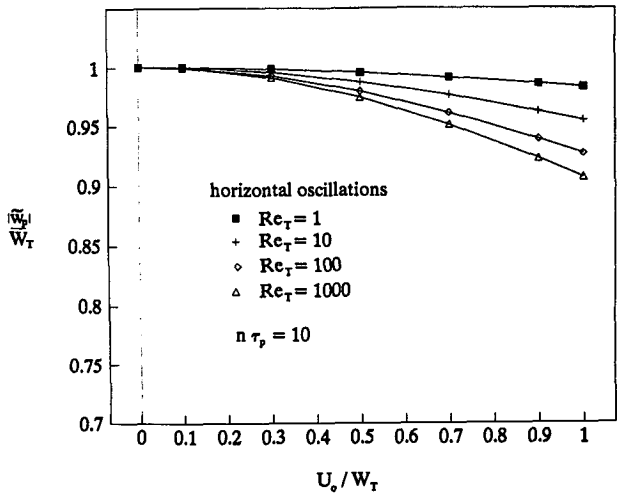

FIG. 9. Cycle-averaged settling velocity within a horizontally oscillating fluid as a function of scaled oscillation amplitude and Re_T.

This is consistent with the fact that drag becomes increasingly nonlinear with increasing Re_T.

b. *Horizontally oscillating fluid*

In this case we set the vertical fluid velocity to zero and allow the horizontal component to vary with time as

$$u = U_0 \sin(2\pi n t). \tag{20}$$

A typical time trace for $U_0/W_T = 0.5$ and $n\tau_p = 10$ is shown in Fig. 7b. Again we see an adjustment to a settling velocity that is less than the still air value, but the horizontal fluid oscillations clearly have less effect on the settling velocity than the same amplitude vertical oscillations.

To determine the sensitivity of the settling velocity to the amplitude of horizontal fluid oscillations, the model was run for $0 \leq U_0/W_T \leq 1$, and the results are shown in Fig. 9. As in the previous case, the magnitude of the settling velocity decreases with increasing amplitude U_0/W_T and increasing Re_T. However, the reduction of settling velocity due to horizontal fluid oscillations is significantly less than that for the same amplitude vertical fluid oscillations. Recall that the vertical component of drag is proportional to $C_D V_{rel} w_{rel}$. Note that u_{rel}, produced by horizontal oscillations, appears only in the term V_{rel} whereas w_{rel}, produced by vertical oscillations, appears twice. Thus, one might expect that vertical oscillations will have a more significant effect on vertical motion than will horizontal oscillations.

c. *Effect of oscillation frequency*

If the period of fluid velocity oscillation n^{-1} is much smaller than the particle response time τ_p, then the particle cannot fully react or adjust to each fluid oscillation. On the other hand, if the period of fluid oscillation is much larger than the particle response time, then the particle tends to more closely follow the fluid motions. A measure of the relative timescales for the fluid and particle is expressed by the product $n\tau_p$. The response of particles to the relative frequency of fluid oscillations was determined through a series of numerical experiments in which the cycle-averaged settling velocity was determined for $Re_T = 100$ and either $U_0/W_T = 0.5$ or $W_0/W_T = 0.5$.

The results, shown in Fig. 10, reveal that if $n\tau_p > 1$, the cycle-averaged settling velocity is nearly indepen-

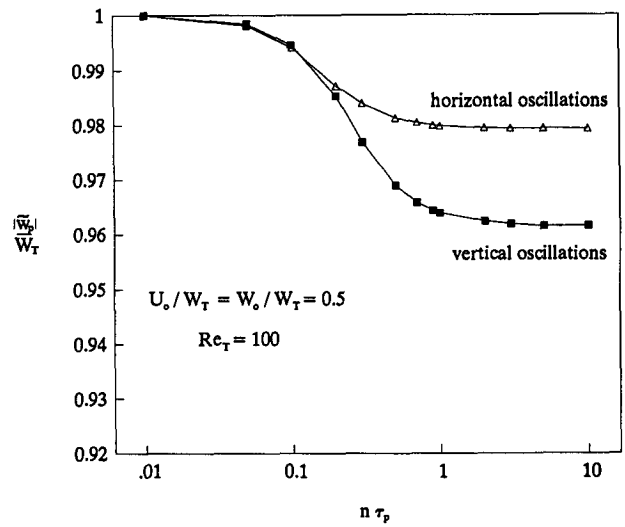

FIG. 10. Cycle-averaged settling velocity within either a horizontally or vertically oscillating fluid as a function of scaled oscillation frequency $n\tau_p$.

dent of oscillation frequency for either horizontal or vertical fluid oscillations. For such high relative frequencies there is a lack of coincidence between the motion of the particle and fluid. As a result, the settling velocity depends only on the amplitude of the oscillations. As the oscillation frequency is reduced such that $n\tau_p < 1$, the settling velocity slowly returns to the still air value. At such low relative frequencies the particle tends to simply drift with the fluid, and relative velocity perturbations are reduced. The nonlinear drag effect appears to virtually vanish for $n\tau_p < 0.01$.

d. Conclusions

In conclusion we can state that the greater the magnitude of fluid velocity oscillation, the greater is the reduction of settling velocity. For the same amplitude of oscillations ($U_0 = W_0$), a larger settling velocity reduction occurs if the fluid oscillates vertically as opposed to horizontally. For $n\tau_p > 1$ the cycle-averaged settling velocity becomes independent of fluid oscillation frequency. For $n\tau_p < 1$, the nonlinear drag effect decreases with decreasing frequency and, for practical purposes, vanishes at $n\tau_p < 0.01$.

Within a turbulent flow a particle experiences many fluid velocity fluctuations of differing frequency, magnitude, direction, and duration. Thus, a fluid oscillating in only one direction is a fairly crude model of turbulence. Nevertheless, it does provide interesting insight into the mechanisms involved in modification of particle settling velocity.

6. Isotropic turbulence

Within a turbulent flow prediction of particle motion is limited by our incomplete knowledge of the time history of fluid motions. Often turbulence statistics are known, from which one must attempt to extract a reasonable simulation of the time history of fluid velocity fluctuations. Past attempts at simulating turbulence involve techniques such as direct numerical simulation (Ueda et al. 1983), large eddy simulation (Deardorff 1972; Yeh and Lei 1991), random Fourier modes (Fung et al. 1992), and Markov chain methods (Smith 1968; Ley 1982).

There is no perfect technique for simulating turbulence; each method has advantages as well as major shortcomings. Direct numerical simulation is limited to low Reynolds number flows. Large eddy simulation can adequately describe the large-scale features of the flow field but cannot resolve small eddies. Stochastic models based upon the random Fourier modes technique or the Markov chain technique do not suffer this limitation but they cannot accurately describe large-scale coherent structures.

Stochastic models of turbulence are computationally efficient when used to simulate the motion of particles since they can provide the fluid velocity at the position of a particle. Turbulence obtained from either the large eddy simulation or the direct numerical simulation require interpolation between grid points to determine the velocity at the position of a particle. The Markov chain technique is perhaps the simplest stochastic technique and it provides a reasonable simulation of turbulence that corresponds to prescribed turbulence statistics. The simplicity of the model and the resulting high speed of computation allow many cases to be run within a short time period. This practical advantage is important since it allows for a detailed series of numerical experiments.

In this paper, we apply a three-dimensional Markov chain model for predicting fluid velocities in isotropic turbulence. The fluid velocity is predicted at successive positions along the particle path. The particle response is obtained by numerically integrating the equation of motion as expressed in Eq. (18).

a. Fluid velocity equations

The instantaneous fluid velocity vector is a sum of mean flow and turbulent fluctuations,

$$\mathbf{V} = \bar{\mathbf{V}} + \mathbf{v}, \tag{21}$$

where the turbulent fluctuation vector has components $\mathbf{v} = (u, v, w)$.

The fluid velocity at the current position of the particle is assumed to be correlated to the fluid velocity at the previous position plus a random fluctuation due to turbulence. Following Smith (1968), we write each fluid velocity component as a Markov chain:

$$u_{\tau+1} = R_{uu}u_\tau + \epsilon_{\tau+1}\sigma(1 - R_{uu}^2)^{1/2}, \tag{22}$$

$$v_{\tau+1} = R_{vv}v_\tau + \theta_{\tau+1}\sigma(1 - R_{vv}^2)^{1/2}, \tag{23}$$

$$w_{\tau+1} = R_{ww}w_\tau + \eta_{\tau+1}\sigma(1 - R_{ww}^2)^{1/2}, \tag{24}$$

where the subscripts τ and $\tau + 1$ denote time steps along the particle pathline and the autocorrelation coefficients R_{uu}, R_{vv}, and R_{ww} are functions of the time step Δt.

The random components ϵ, θ, and η are generated in a two-step process by first generating a uniform deviate between 0 and 1 using a modulo technique discussed by Hamming (1962), then transforming the uniform distribution to a Gaussian distribution using a technique developed by Box and Muller (1958). In isotropic turbulence there is a zero-mean fluid velocity, constant standard deviation σ, and a zero cross-correlation; thus, the random components must have zero-mean unit standard deviation, and the random values must be independently generated.

The autocorrelations of fluid velocities between successive positions are functions of both the mean distance and elapsed time between particle positions. We adopt the formulation of Csanady (1963)

for the correlation functions for falling heavy particles

$$R_{uu}(\Delta t) = R_{vv}(\Delta t) = \left(1 - \frac{1}{2}\frac{W_T}{\sigma}\frac{\Delta t}{T_L}\right)e^{-\Delta t/T}, \quad (25)$$

and

$$R_{ww}(\Delta t) = e^{-\Delta t/T}, \quad (26)$$

where

$$T = \frac{T_L}{\left(1 + \frac{W_T^2}{\sigma^2}\right)^{1/2}}. \quad (27)$$

Note that as the ratio $\sigma/W_T \to \infty$ then $T \to T_L$.

b. Frequency spectrum

In the previous section we consider a fluid oscillating at a single frequency, so that the frequency spectrum consists of a single Dirac delta function. In turbulence the fluid oscillations are distributed over a broad range of frequencies. The frequency spectrum of fluid motions is obtained by taking the Fourier transform of the autocorrelation function as follows:

$$S(n) = 4\int_0^\infty R(t/T_L)\cos(2\pi n t)dt. \quad (28)$$

The frequency spectrum as seen by a falling particle, $S_p(n)$, is obtained by substituting Eq. (26) into Eq. (28). Integration yields $S_p(n)$, which can be written in nondimensional form as

$$\frac{\pi n S_p(n)}{\sigma^2} = \frac{4\pi n T_L\left(1 + \frac{W_T^2}{\sigma^2}\right)^{1/2}}{1 + \frac{W_T^2}{\sigma^2} + 4\pi^2 n^2 T_L^2}. \quad (29)$$

In turn $S_p(n)$ reduces to the Lagrangian fluid velocity spectrum $S(n)$ as the terminal velocity approaches zero or as $\sigma/W_T \to \infty$, where $S(n)$ is

$$\frac{\pi n S(n)}{\sigma^2} = \frac{4\pi n T_L}{1 + 4\pi^2 n^2 T_L^2}. \quad (30)$$

In this paper we are considering the case of large and heavy particles where $\sigma/W_T < 1$, so this simplification is not possible. A plot of the Lagrangian frequency spectrum $S(n)$ is shown in Fig. 11 with $S_p(n)$ calculated for $\sigma/W_T = 0.1$ and 0.5. Clearly a falling particle will experience a frequency spectrum shifted toward higher frequencies.

The spectral peak of $S_p(n)$ is denoted n_{mp} and may be expressed as

$$n_{mp} = \frac{\left(1 + \frac{W_T^2}{\sigma^2}\right)^{1/2}}{2\pi T_L}. \quad (31)$$

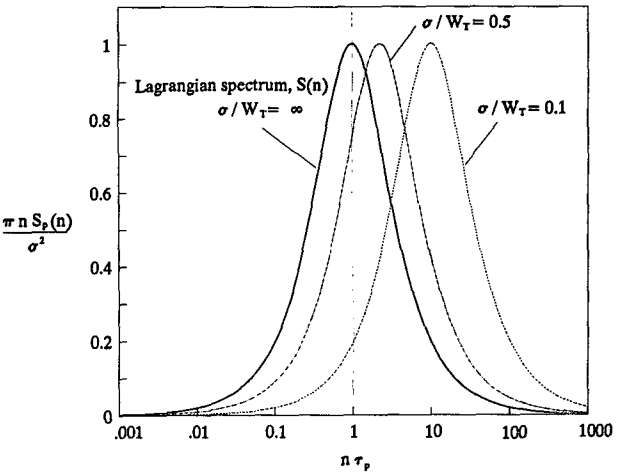

FIG. 11. Lagrangian spectrum compared with the shifted spectrum of a falling particle.

If the particle is not falling through the turbulent field, that is, $W_T = 0$, then we have a Lagrangian particle, and the peak in the Lagrangian velocity spectrum n_{mL} is

$$n_{mL} = \frac{1}{2\pi T_L}. \quad (32)$$

The ratio of the spectral peaks n_{mp}/n_{mL} is thus

$$\frac{n_{mp}}{n_{mL}} = \left(1 + \frac{W_T^2}{\sigma^2}\right)^{1/2}. \quad (33)$$

As shown in Fig. 11, for $\sigma/W_T = 0.1$ the peak in the spectrum is shifted by one full decade, whereas for $\sigma/W_T = 0.5$ the frequency shift is significantly less.

c. Numerical simulations of settling velocity

Generally, the motion of a particle depends upon three independent dimensionless parameters: Re_T, σ/W_T, and T_L/τ_p. The last two parameters are used to obtain the frequency spectrum as seen by a falling particle $S_p(n)$.

Each particle is released with no horizontal motion and with a vertical velocity equal to the still air terminal velocity. The motion of each particle is obtained by numerically solving the equations of motion as expressed in Eq. (18), with the fluid velocity calculated from the stochastic velocity equations. The final settling velocity is defined as the ensemble average velocity for 1000 particles. The particles are allowed to fall for a time of at least five particle time constants to allow sufficient time for their motion to become independent of the initial conditions and so that they have time to adjust fully to the simulated field of turbulence.

The time step for computation is constrained by separate, and sometimes conflicting, criteria. First, it is

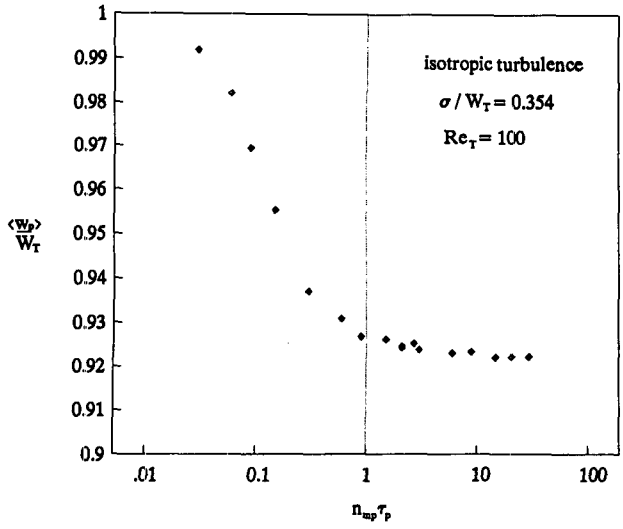

FIG. 12. Ensemble-averaged settling velocity within simulated isotropic turbulence as a function of the scaled spectral peak frequency.

necessary to maintain the ratio of the time step to the Lagrangian integral timescale at a value less than unity $\Delta t/T_L < 1$ (Wilson and Zhuang 1989). For the particle dynamics model to perform properly the time step should be less than the particle time constant $\Delta t/\tau_p < 1$. On the other hand, the exponential form of the autocorrelation function is not strictly valid for $\Delta t/T_L \ll 0.01$. Thus, the time step is constrained by $0.01 \ll \Delta t/T_L \ll 1$. For very low frequencies (where T_L is large) both criteria cannot be satisfied simultaneously. When possible, we maintained a constant $\Delta t/T_L = 0.1$ and always maintained $\Delta t/\tau_p < 1$.

d. *Sensitivity of settling velocity to n_{mp}*

We intend here to ascertain the effects of frequency on the settling velocity of a particle in simulated isotropic turbulence. As discussed earlier, the spectrum of fluid velocity fluctuations following the particle motion is defined by σ, T_L, and W_T. All three parameters determine the spectrum peak frequency n_{mp}. For this series of numerical experiments we vary n_{mp} by systematically varying T_L while maintaining a fixed value of $\sigma/W_T = 0.354$ (the same value used for the sinusoidally oscillating fluid). The only other dimensionless parameter required to run the model is the terminal Reynolds number, which for this set of calculations is held constant at $\mathrm{Re}_T = 100$.

The results, plotted in Fig. 12, show the effect of varying n_{mp} on the resulting ensemble-averaged settling velocity. Similar to the previous case of the oscillating fluid, we find that the average settling velocity in isotropic turbulence is less than that in still fluid. For $n_{mp}\tau_p > 1$, the average settling velocity becomes independent of frequency, since the particle is not given sufficient time to respond to the series of turbulent gusts that it encounters. In this regime the average settling velocity is only a function of σ/W_T and Re_T. On the other hand, for $n_{mp}\tau_p < 1$, the reduction of settling velocity gradually decreases with decreasing frequency until it vanishes somewhere near $n_{mp}\tau_p < 0.01$.

In the oscillating fluid case the contribution to the variance is contained in a single frequency and this nondimensional frequency $n\tau_p$ is either greater than or less than unity. In isotropic turbulence the spectrum, as depicted in Fig. 11, spans a range of frequencies. When $n_{mp}\tau_p$ is near unity, a part of the contribution to the variance is contained in frequencies greater than unity and the remaining part is contained in frequencies less than unity. The part of the spectrum with $n\tau_p < 1$ contributes considerably less to the slowing of particle settling velocity than does the part of the spectrum where $n\tau_p > 1$.

e. *Sensitivity of settling velocity to σ/W_T*

For $n_{mp}\tau_p > 1$, the average settling velocity becomes virtually independent of T_L/τ_p and so depends only upon Re_T and σ/W_T. In the next series of experiments we varied σ/W_T from 0.0 to 0.8 for several values of Re_T and $n_{mp}\tau_p = 10$. The results, plotted in Fig. 13, show separate curves for $\mathrm{Re}_T = 1$, 10, 100, and 1000. The results reveal that the settling velocity tends to decrease with increasing σ/W_T. A reduction greater than 35% is found for $\sigma/W_T = 0.8$ and $\mathrm{Re}_T = 1000$. The rate of settling velocity reduction decreases with decreasing Re_T, as drag nonlinearity decreases, and it vanishes within the Stokes regime.

Compared with the simple oscillating fluid, the velocity reduction in isotropic turbulence is somewhat greater. Perhaps this is because in isotropic turbulence

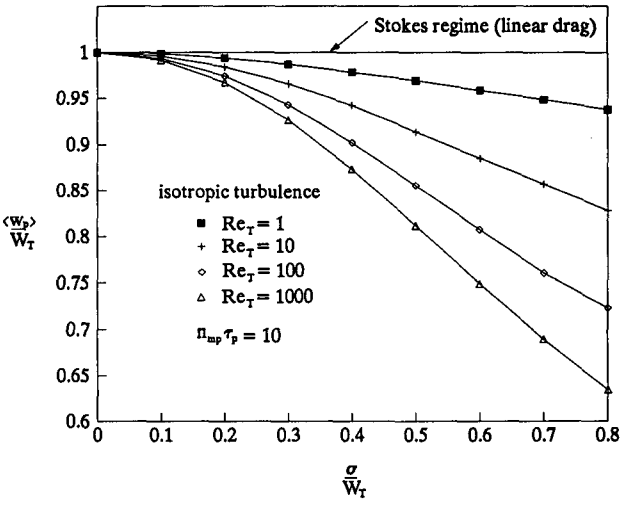

FIG. 13. Ensemble-averaged settling velocity within simulated isotropic turbulence as a function of σ/W_T and Re_T.

we have both horizontal and vertical components of relative velocity simultaneously contributing to the nonlinear drag effect, whereas for the oscillating fluid case we considered horizontal and vertical oscillations separately.

f. Conclusions

We conclude that there is a significant reduction of the average settling velocity for particles experiencing nonlinear drag while falling through isotropic turbulence. Settling velocity reduction generally depends upon three independent dimensionless parameters: Re_T, σ/W_T, and T_L/τ_p. For a constant value of Re_T and σ/W_T, the average settling velocity becomes independent of frequency when $n_{mp}\tau_p > 1$. When $n_{mp}\tau_p < 1$, the nonlinear drag effect gradually decreases with decreasing frequency until it is negligible below $n_{mp}\tau_p \approx 0.01$. In the region of frequency independence the settling velocity tends to decrease with increasing σ/W_T as well as with increasing Re_T.

Acknowledgments. This research has been supported by the U.S. Environmental Protection Agency under the Cooperative Agreement CR 817931 with North Carolina State University. The contents of this paper do not necessarily reflect the views and policies of the Agency, nor does mention of trade names or commercial products constitute endorsement or recommendation for use.

APPENDIX

Time History of Fall

a. Overview

In this section formulas are derived for the prediction of the time history of particle velocity when falling through still fluid. In section b we review the well-known formula for a particle undergoing linear drag forces within the Stokes regime (Fuchs 1964). In section c we consider a particle in the nonlinear drag regime.

Consider the motion of a particle released with no horizontal relative motion within a steady and homogeneous fluid. In this case $u_{\mathrm{rel}} = v_{\mathrm{rel}} = 0$ and the equation of particle motion reduces to

$$\frac{dw_{\mathrm{rel}}}{dt} = g\frac{\rho_p - \rho}{\rho_p} - \frac{3}{4}\frac{\rho}{\rho_p}\frac{C_D}{D}|w_{\mathrm{rel}}|w_{\mathrm{rel}}. \quad \text{(A1)}$$

It is more convenient to work with the nondimensional form of the governing equation of motion. Selecting the particle time constant $\tau_p = W_T/[g(\rho_p - \rho)/\rho_p]$ as a timescale and the terminal velocity W_T as a velocity scale, we define the following scaled variables:

$$t^* = \frac{t}{\tau_p}, \quad w^*_{\mathrm{rel}} = \frac{w_{\mathrm{rel}}}{W_T}. \quad \text{(A2)}$$

The equation of motion may be rewritten in the following nondimensional form:

$$\frac{dw^*_{\mathrm{rel}}}{dt^*} = 1 - \frac{C_D}{C_{D_T}}|w^*_{\mathrm{rel}}|w^*_{\mathrm{rel}}. \quad \text{(A3)}$$

b. Solution for the Stokes regime (linear drag)

Within the Stokes drag regime $C_D/C_{DT} = |w^*_{\mathrm{rel}}|^{-1}$ and the equation of particle motion reduces to

$$\frac{dw^*_{\mathrm{rel}}}{dt^*} = 1 - w^*_{\mathrm{rel}}. \quad \text{(A4)}$$

Integration of this equation from an initial value of w^*_{relo} yields the solution

$$w^*_{\mathrm{rel}}(t^*) = 1 + (w^*_{\mathrm{relo}} - 1)e^{-t^*}. \quad \text{(A5)}$$

This equation is valid for both positive and negative initial values of w^*_{relo}. If the particle is released with no initial relative motion, then Eq. (A5) reduces to the well-known equation (e.g., Fuchs 1964):

$$w^*_{\mathrm{rel}}(t^*) = 1 - e^{-t^*}. \quad \text{(A6)}$$

c. Solution for nonlinear drag

Ignoring the variation of the drag coefficient as the particle accelerates by making the approximation $C_D = C_{DT}$, we get

$$\frac{dw^*_{\mathrm{rel}}}{dt^*} = 1 - |w^*_{\mathrm{rel}}|w^*_{\mathrm{rel}}. \quad \text{(A7)}$$

For heavy particles released with a positive initial value of the vertical relative velocity $w^*_{\mathrm{relo}} \geq 0$, we need only consider positive value of w^*_{rel}; thus,

$$\frac{dw^*_{\mathrm{rel}}}{dt^*} = 1 - w^{*2}_{\mathrm{rel}}. \quad \text{(A8)}$$

Integration of this equation from a positive initial value of w^*_{relo} yields the solution

$$w^*_{\mathrm{rel}}(t^*) = \frac{e^{t^*} - \left(\dfrac{1 - w^*_{\mathrm{relo}}}{1 + w^*_{\mathrm{relo}}}\right)e^{-t^*}}{e^{t^*} + \left(\dfrac{1 - w^*_{\mathrm{relo}}}{1 + w^*_{\mathrm{relo}}}\right)e^{-t^*}}. \quad \text{(A9)}$$

If the particle is released with no initial relative motion, then this equation reduces to

$$w^*_{\mathrm{rel}}(t^*) = \tanh(t^*). \quad \text{(A10)}$$

REFERENCES

Box, G. E. P., and M. E. Muller, 1958: A note on the generation of random normal deviates. *Ann. Math. Stat.*, **28**, 610–611.

Clift, R., J. R. Grace, and M. E. Weber, 1978: *Bubbles, Drops, and Particles.* Academic Press, 380 pp.

Csanady, G. T., 1963: Turbulent diffusion of heavy particles in the atmosphere. *J. Atmos. Sci.*, **20**, 201–208.

Deardorff, J. W., 1972: Numerical investigation of neutral and unstable planetary boundary layers. *J. Atmos. Sci.*, **29,** 91–115.

Fuchs, N. A., 1964: *The Mechanics of Aerosols.* Pergamon Press, 408 pp.

Fung, J. C. H., J. C. R. Hunt, N. A. Malik, and R. J. Perkins, 1992: Kinematic simulation of homogeneous turbulence by unsteady random Fourier modes. *J. Fluid Mech.*, **236,** 281–318.

Gunn, R., and G. D. Kinzer, 1949: The terminal velocity of fall for water droplets in stagnant air. *J. Meteor.*, **6,** 243–249.

Hamming, R. W., 1962: *Numerical Methods for Scientists and Engineers.* McGraw-Hill, 411 pp.

Kladas, D. D., and D. P. Georgiou, 1993: A relative examination of C_D–Re relationships used in particle trajectory calculations. *ASME J. Fluids Eng.*, **115,** 162–165.

Laws, J. O., 1941: Measurements of the fall velocity of water drops and rain drops. *Trans. Amer. Geophys. Union,* **22,** 709–721.

Ley, A. J., 1982: A random walk simulation of two-dimensional turbulent diffusion in the neutral surface layer. *Atmos.–Environ.,* **16,** 2799–2808.

Manton, M. J., 1974: On the motion of a small particle in the atmosphere. *Bound.-Layer Meteor.*, **6,** 487–504.

Mason, B. J., 1957: *The Physics of Clouds.* Oxford University Press, 481 pp.

Maxey, M. R., 1987: The gravitational settling of aerosol particles in homogeneous turbulence and random flow fields. *J. Fluid Mech.*, **174,** 441–465.

——, and S. Corrsin, 1986: Gravitational settling of aerosol particles in randomly oriented cellular flow fields. *J. Atmos. Sci.*, **43,** 1112–1134.

Schöneborn, P.-R., 1975: The particle interaction between a single particle and an oscillating fluid. *Int. J. Multiphase Flow.* **2,** 307–317.

Smith, F. B., 1968: Conditioned particle motion in a homogeneous turbulent field. *Atmos.–Environ.*, **2,** 491–508.

Stommel, H., 1949: Trajectories of small bodies sinking slowly through convection cells. *J. Mar. Res.*, **8**(1), 24–29.

Stout, J. E., Y.-L. Lin, and S. P. S. Arya, 1993: A theoretical investigation of the effects of sinusoidal topography on particle deposition. *J. Atmos. Sci.*, **50,** 2533–2541.

Tunstall, E. B., and G. Houghton, 1968: Retardation of falling spheres by hydrodynamic oscillations. *Chem. Eng. Sci.*, **23,** 1067–1081.

Ueda, T., K. Jinno, K. Momii, and K. Maehama, 1983: Numerical study of diffusivity of settling particles in homogeneous isotropic turbulence. *Trans. Japan. Soc. Civ. Eng.*, **15,** 293–296.

Wang, L.-P., and M. R. Maxey, 1993: Settling velocity and concentration distribution of heavy particles in homogeneous and isotropic turbulence. *J. Fluid Mech.*, **256,** 27–68.

White, F. M., 1974: *Viscous Fluid Flow.* McGraw-Hill, 725 pp.

Wilson, J. D., and Y. Zhuang, 1989: Restriction on the time step to be used in stochastic Lagrangian models of turbulent diffusion. *Bound.-Layer Meteor.*, **49,** 309–316.

Yeh, F., and U. Lei, 1991: On the motion of small particles in a homogeneous isotropic turbulent flow. *Phys. Fluids A,* **3,** 2571–2586.

Zahm, A. F., 1926: Flow and drag formulas for simple quadrics. NACA Tech. Rep. 253, 517–537.